International Journal of ChemTech Research
CODEN (USA): IJCRGG, ISSN: 0974-4290, ISSN(Online):2455-9555
Vol.10 No.3, pp 515-529, 2017

Inhibition and Adsorption Actions of Nano Curcumin for Corrosion of Carbon Steel Alloy in 3.5% NaCl Solution

Khulood Abid Saleh[1], Mays Khalid Mohammed[2]*

[1,2] University of Baghdad/ Collage of Science/ Department of Chemistry, Baghdad, Iraq.

Abstract : The corrosion inhibition of carbon steel in 3.5% NaCl solution by nano curcumin has been studied at temperature range (298-328K) and different concentrations ($2.7*10^{-6}$, $1.3*10^{-5}$,$2.7*10^{-5}$ and $4.1*10^{-5}$ M) using potentiostatic techniques. The obtained data shows that the corrosion rate increase with temperature increase at all nano curcumin concentrations, also it decrease with nano curcumin concentration increase up to $2.7*10^{-5}$ M then with increasing nano curcumin concentration more than $2.7*10^{-5}$ M the corrosion rate will increase. The results showedthat the best inhibition efficiency obtained with $2.7*10^{-5}$ M nano curcumin concentration which equal to 86.21% at 298K. The Kinetics (Apparent activation energy E_a, arrhenius factor A) and Thermodynamics (free energy ΔG^*, enthalpy ΔH^* and entropy ΔS^* of activation) parameters for corrosion processes were calculated. Study the adsorption behavior of nano curcumin inhibitor by adsorption isotherm has been done and values of K_{ads} , ΔH_{ads} , ΔS_{ads} and ΔG_{ads} for adsorption process were calculated. The adsorption of nano curcumin on carbon steel surface is chemisorption type and it obey Langmuir adsorption isotherm. Nano curcumin inhibitor powder and the adsorbed layer on C.S surface in the best inhibition efficiency and best temperature were analyzed by AFM and FTIR spectra in order to study the change in particles size and functional groups respectively.
Keywords : Corrosion, Corrosion Inhibitors, Nano Curcumin, Langmuir Adsorption Isotherm.

1. Introduction

Corrosion is the destructive attack of a metal by chemical or electrochemical reaction with its environment [1]. Among the various methods to avoid or prevent destruction or degradation of metal surface, the usage of corrosion inhibitors is one of the best known methods of corrosion protection in engineering industry. This method is following stand up due to low cost and practice method [2-4]. Corrosion inhibitors can be defined as chemicals, either organic or inorganic, which when added in small amounts to a corroding system, significantly reduce the corrosion rate of the metal/alloy concerned, therefore, they provide corroding surfaces, with some levels of protection by either forming a film there on or reacting with the corroding surface to form inert compounds [5].

Turmeric (figure 1) is a short stemmed perennial, which grows to up to 100 cm in height. It has curved, oblong, and ovate leaves with beautiful white to colorful flower and cylindrical rhizomes [6].

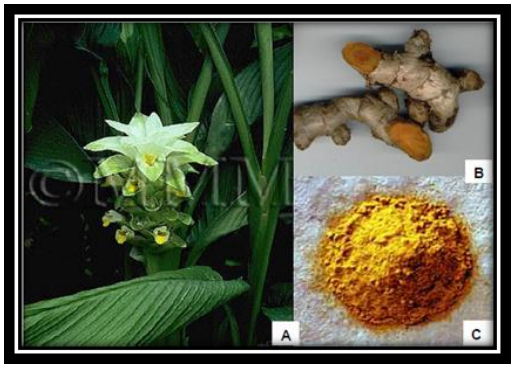

Figure 1. A) Turmeric Plant with flower, B) Freshly cut rhizome and C)Turmeric rhizome dried powder.

The most active component of turmeric is curcumin (figure 2) and it's chemical name is 1,7-bis(4-hydroxy-3-methoxyphenyl)-1,6-heptadiene-3,5 dione which is a bis-α,β-unsaturated β-diketone [7].

Figure 2. Chemical structure of curcumin.

Nano curcumin (N.C) has recently been used in medicine, because of the clinical application of curcumin is severely limited by its main drawbacks such as instability, low solubility, poor bioavailability and rapid metabolism [8]. So the researches focused to convert curcumin to nano curcumin in order to improve the solubility of curcumin in water mainly, among these researches the usage of nano curcumin to treat the pancreatic cancer [9].

The aim of this study was to investigate the effectiveness of nano curcumin with some additives (SDS, NaOH and Acetone) as organic corrosion inhibitor for carbon steel (C.S) in 3.5% NaCl solution at temperature range (298 - 328 K) using Potenstatic measurements. The nano curcumin in this study was prepared from pure curcumin.

2. Experimental Part

2.1. Chemicals and Materials:

Carbon Steel (C.S) was used as metallic materials with chemical Composition as described in the table (1).

Table 1. chemical composition for carbon steel (C45).

Grad	*% C*	*% Si*	*% Mn*	*%S*	*% P*	*% Ni*	*% Cr*	*%Mo,*	*%Fe*
C45	0.42-	<0.40	0.50-	<0.045	<0.045	0.40	<0.40	<0.10	97.31-97.69

Many chemical were used in this work include some regents which are listed in table (2) with their purity and origin.

Table 2. Chemical materials used in this study.

Raw Material	***Molecular Formula***	***Supplier***	***Purity***
Distilled Water	H_2O	University of Baghdad/College of Science.	1 μ.S
Sodium dodecyl sulfate (SDS)	$NaC_{12}H_{25}SO_4$	Fluka	99%
Sodium hydroxide	NaOH	BDH	96%
Acetone	CH_3COCH_3	AFCO Jordan	99.5%
Sodium Chloride	NaCl	MERCK	99.5%
Pure Curcumin	$C_{21}H_{20}O_6$	Fluka	98%

2.2. Preparation of Specimen

A piece of carbon steel (C45) of (0.5 mm) thickness was mechanically cut in to circular sample with dimensions of 2.5 cm in diameter then: Carbon steel sample surface was polished with silicon carbaid paper in different sizes (320, 400, 800, 1000, 1200, 1500, 2000) until it gain a mirror image shape.Then washed by distilled water and acetone. The Specimen was kept in desiccators for protecting and preventing them from oxidation by atmospheric air and moisture.

2.3. Preparation of Nano Curcumin, Test and Inhibiting Solution:

- Preparation of nano curcumin:

Nano curcumin was prepared using Top-down approach, in which the poor water soluble curcumin is dissolved in a non-polar solvent (acetone) then added to polar solvent (distilled water) to form precipitate.

The method of preparation is stepped bellow:-

1) Two solution was prepared:

a) 200 mg of pure curcumin was dissolved in 10 ml of acetone.
b) 300 mg of SDS was dissolved in 100 ml of distilled water which was kept on a magnetic stirrer for continuous stirring.

2) Then the solution (a) was added drop wise to solution (b), finally obtained bright orange color solution (figure 3 A) .

3) The prepared nano curcumin solution than completely dissolved by 0.075 g of NaOH (figure 3 B) to obtain a black red solution, then complete the volume to 1 litter using distilled water so we obtained $5.4*10^{-4}$ M of nano curcumin solution.

SDS was used as stabilizer and the stability of above solutions up to four week [10].

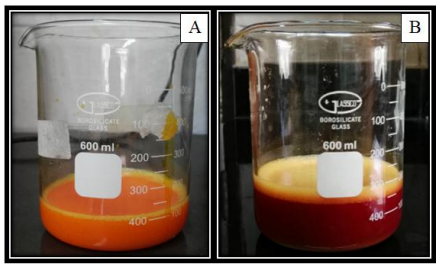

Figure 3. A) bright orange color of prepared nano curcumin solution, B) Dark red color of dissolving nano curcumin in NaOH.

• Preparation of test solution:

2.5 ml of aceton,0.075 g of SDS, 0.0187 g of NaOH and 35g of NaCl have been added and complete the volume to 1 litter by distilled water in order to prepare the test solution (as a blank solution).

• Preparation of inhibiting solution:

250 ml has been taken from the prepared nano curcumin ($5.4*10^{-4}$ M) and complete the volume to 1 litter using distilled water in order to prepare the stock solution ($1.3*10^{-4}$ M), Then prepare ($2.7*10^{-6}$, $1.3*10^{-5}$, $2.7*10^{-5}$, $4.1*10^{-5}$ M) nano curcumin inhibiting solutions from the stock solution then added 35 g NaCl to each concentration and finally complete the volume to 1 litter using distilled water.

2.4. Electrochemical Measurements

In this technique three electrode corrosion cell was used, in which the working electrode is carbon steel (type:C45), the reference electrode is the standard Calomel electrode and the auxiliary electrode is platinum electrode. The electrochemical system consists of potentiostate device (Germany, Mlab 2000), corrosion cell (1000 mL) and electrodes with a computer and MLabSci software were used for data acquisition and analysis [11]. And finally it consist of water bath to control the temperature.

To determine the open circuit potential (OCP) of the specimens, the specimens have been immersed in the blank solution (3.5% NaCl, SDS, NaOH and acetone) in different temperatures (298, 308, 318 & 328K) to reach the steady state between the specimen material and electrolytic solution. The change in potential according to the current were determined during (15 min.), and time step equal to 60 seconds for each specimens. After reaching the steady state condition, the determined potential is known as corrosion potential or free potential or open circuit potential.

3. Results and Discussion

3.1. Potentiostatic polarization measurements

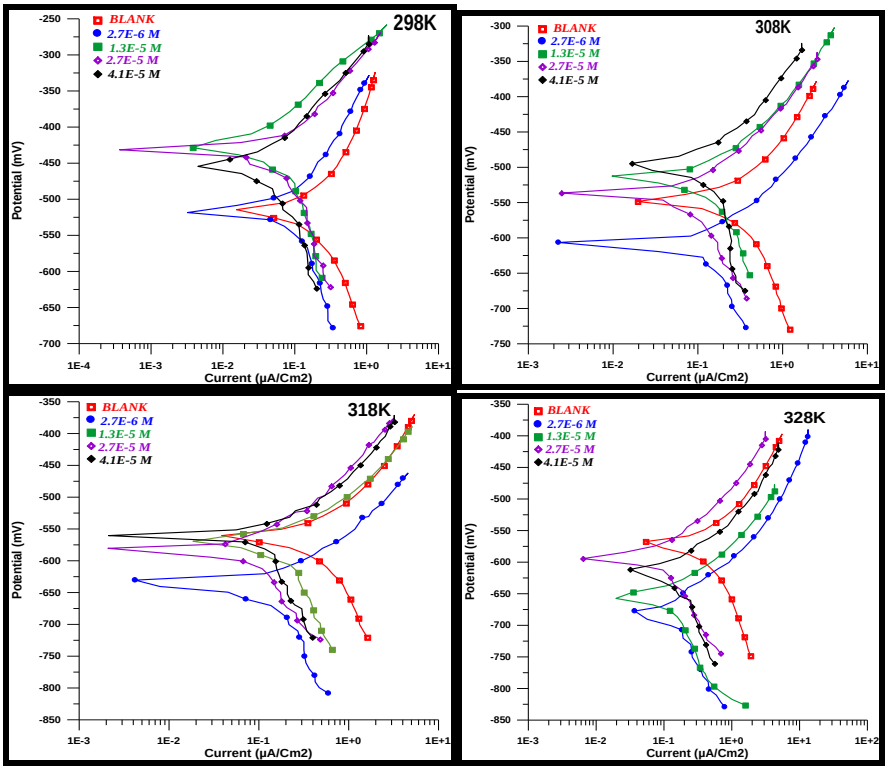

Figure 4. Polarization plots of C.S corrosion in 3.5% NaCl and additives for various concentrations of nano curcumin inhibitor at temperature range 298-328K.

The potentiostatic polarization curves for the corrosion of carbon steel in uninhibited and inhibited 3.5% NaCl solution with the additives (SDS, NaOH, acetone) were involved in the nano curcumin preparing solution, in temperatures range (298-328)K are shown in figure (4).

Figure (4) shows, that the corrosion potential has been shifted in the presence of (N.C) compared with it is absence to less negative values that's mean the C.S alloy become more noble toward corrosion process in the presence of all inhibitor concentration at 298K also C.S shows similar effect at 308 K except 2.7 $*10^{-6}$ M (N.C) concentration in which the corrosion potential shift to more negative value and become more active toward corrosion process , in other hand, the corrosion potential shift to more negative values at 318 K and 328 K at all (N.C) inhibitor concentrations, also the corrosion current densities reduce in the presence of (N.C) inhibitor.

The extrapolation method for the polarizations curves was applied and the data of corrosion potential (E_{corr}), corrosion current density (i_{corr}), cathodic and anodic Tafel slopes (b_c and b_a) , weight loss (W.L), penetration loss (P.L) and percentage of inhibition efficiency (%IE) are listed in (table 3).

Inhibition efficiency (%IE) can be determine using the following equation[12]:

$$\%IE = \frac{i - i_{in}}{i} \times 100 \qquad \text{....(1)}$$

Where iand i_{in} are the corrosion current densities in the absence and presence of the inhibitor, respectively.

The polarization resistance (R_P) may best determined from the following equation [12].

$$R_p = \frac{b_a b_c}{2.303\,(b_a + b_c) i_{corr}} \qquad \text{.... (2)}$$

Where: i_{corr} in $A.cm^{-2}$, ba, bc are in $V.dec^{-1}$ and R_P in $\Omega.\ cm^2$.

For engineering requirements the corrosion current density units have been converted from ($\mu A.cm^{-2}$) unit to milli-inch per year (mpy) by using the following equation:

$$R\ (mpy) = 0.13 * i_{corr} * \frac{e}{\rho} \qquad \text{.... (3)}$$

Where R is the corrosion rate in mpy units, i_{corr} is the corrosion current density in $mA.cm^{-2}$, ρ is the C.S density which equal to 7.87 g/cm^3, e is the chemical equivalent weight of the C.S.

The corrosion kinetic parameters which obtained from the polarization curves are given in table (3), in which the polarization resistance, inhibition efficiency and corrosion rate in (mpy) units have been calculated from the equations 1,2 and 3 respectively.

Table 3. Corrosion data of C.S corrosion in 3.5% NaCl solution in the absence and presence of different (N.C) concentrations at temperature range 298-328 K.

$C_{N.C}$ / M	T/K	i_{corr} / μA .cm^{-2}	E_{corr} / mV	b_c/ mV .dec^{-1}	b_a/ mV .dec^{-1}	W.L/ g.m^{-2} .d^{-1}	P.L/ mm.y^{-1}	R_p/ Ω.cm^2	θ	IE%	R/ mpy
Blank	298	82.67	-514.9	-106.3	86.0	20.70	0.960	249.69	-	-	0.038
	308	112.48	-548.0	-86.0	76.0	28.10	1.310	155.75	-	-	0.052
	318	130.50	-560.9	-74.6	53.0	32.60	1.510	103.10	-	-	0.060
	328	161.68	-570.4	-86.7	58.8	40.40	1.880	94.10	-	-	0.075
2.7*10^{-6}	298	34.43	-517.8	-69.4	73.9	8.61	0.400	451.36	0.583	58.35	0.016
	308	73.03	-605.8	-120.7	70.4	18.30	0.848	264.38	0.351	35.07	0.034
	318	95.17	-630.4	-185.2	65.0	23.80	1.100	219.52	0.271	27.07	0.044
	328	145.06	-676.4	-272.6	97.2	36.30	1.680	214.48	0.103	10.28	0.067
1.3*10^{-5}	298	18.80	-428.7	-73.7	77.2	4.70	0.218	870.85	0.773	77.26	0.008
	308	51.01	-514.2	-94.4	55.8	12.80	0.592	298.53	0.546	54.65	0.023
	318	76.41	-571.5	-92.5	57.6	19.10	0.887	201.72	0.414	41.45	0.035
	328	116.52	-657.8	-203.1	90.1	29.10	1.350	232.58	0.279	27.93	0.054
2.7*10^{-5}	298	11.40	-432.5	-46.1	32.8	2.85	0.132	729.96	0.862	86.21	0.005
	308	34.20	-539.2	-75.8	61.4	8.55	0.397	430.69	0.696	69.59	0.016
	318	56.61	-583.0	-127.5	86.5	14.20	0.657	395.30	0.566	56.62	0.026
	328	91.71	-592.6	-183.6	103.8	22.90	1.060	313.96	0.433	43.28	0.042
4.1*10^{-5}	298	19.68	-456.1	-88.7	76.1	4.92	0.228	903.72	0.762	76.19	0.009
	308	50.59	-496.5	-85.2	66.2	12.60	0.587	319.75	0.550	55.02	0.023
	318	59.32	-561.9	-78.8	58.1	14.80	0.688	244.80	0.545	54.54	0.027
	328	94.52	-610.0	-138.7	68.8	23.60	1.100	211.26	0.415	41.54	0.043

Table (3) shows, that the corrosion current densities increase with temperature increase in the presence and absence of (N.C) inhibitor, and decrease with inhibitor concentrations increase up to 2.7*10^{-5} M, then with increasing the inhibitor concentration more than 2.7*10^{-5} M, the corrosion current densities will increase. The opposite of corrosion current density is the inhibition efficiency and the highest value obtained with 2.7*10^{-5} M (N.C) concentration at 298 K which equal to 86.21%, in the other hand, values of penetration loss and weight loss identical to corrosion current densities in the increasing and decreasing.

The results in table (3) shows, that the polarization resistances in the presence of inhibitor are higher than for case in the absence of it, and the highest value obtained with 4.1*10^{-5} M at 298 K which equal to 903.72 Ω.cm^2 .

The corrosion potential increase as the temperature increase in the presence and absence of (N.C) inhibitor.

In general, the corrosion potential values displacement was less than 85 mV in temperature range (289-328 K) and it is mean that (N.C) inhibitor is a mixed type inhibitor (both anodic and cathodic) with some tendencies to become cathodic inhibitor at 318 and 328 K because of the corrosion potential values increase some times in active direction above 85 mV [13].

3.2. Corrosion Kinetic and Thermodynamic Study

Thermodynamic parameters play an important role in studying the corrosionprotection mechanism.The equation used to calculate the activation parameters of the corrosion process is similar to Arrhenius (equation 4). Moreover, transition state (equation 5) were used [14].

$$\mathbf{Log(I_{corr}) = Log\ A - \frac{E_a}{2.303\,R\,T}} \qquad \text{....(4)}$$

$$\mathbf{Log(I_{corr}/T) = Log\ (K/h) + \frac{\Delta S^*}{2.303R} - \frac{\Delta H^*}{2.303RT}} \qquad \text{....(5)}$$

Where i_{corr} is corrosion current density, E_a is the apparent activation energy, R is the universal gas constant (8.314 J $mol^{-1}.K^{-1}$), T is temperature in Kelvin, A is the Arrhenius pre-exponential factor, h is the Plank's constant (6.626 x 10^{-34} J.s), N is the Avogadro's number (6.022 x 10^{23} mol^{-1}), K is the Boltzmann constant, ΔH^* is the enthalpy ofactivation and ΔS^* is the entropy of activation for corrosion process.

The apparent activation energy (E_a) at optimum concentration of nano curcumin was determined by linear regression between log i_{corr} and 1/T (figure. 5) and the result is shown in table (4).

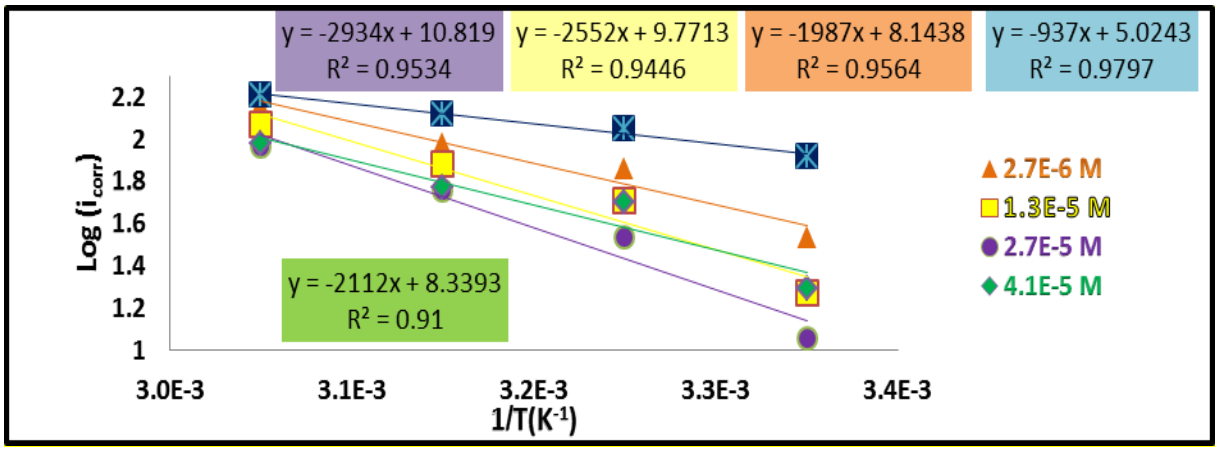

Figure 5. Plot of log i_{corr} versus 1/T for the C.S corrosion in 3.5% NaCl with additives solution containing various (N.C) inhibitor concentrations.

Straight lines were obtained from the plots of log i_{corr}/T vs. 1/T, which are shown in (figure 6). With the slope of ($-\Delta H^*/2.303$ R) and an intercept of[(log (R/Nh) +($\Delta S^*/2.303$ R)] from which the values of ΔH^* and ΔS^*, respectively were calculated.

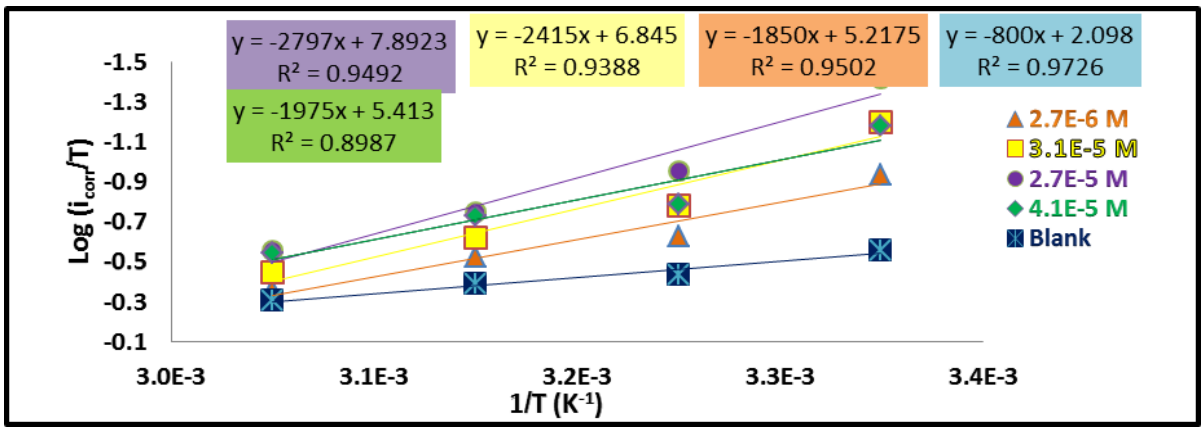

Figure 6. Plots of log i_{corr} /T vs. 1/T for the corrosion of C.S in 3.5%NaCl solution with additives in the presence and the absence of different (N.C) inhibitor concentrations.

By using the estimated values of ΔH^* and ΔS^*, it was possible to calculate the values of the change in Gibbs free energy ΔG^* of activation for corrosion process from the relation:

$$\Delta G^* = \Delta H^* - T\Delta S^* \quad \text{....(6)}$$

The kinetic and thermodynamic quantities are listed in table (4).

Table 4. Activation parameters E_a, ΔH^*, $\Delta S^*$and ΔG^* for the C.S dissolution in 3.5% NaCl solution in the absence and the presence of (N.C) concentrations solutions.

C N.C/ M	T/K	1/T / K^{-1}	i_{corr} /µA.cm^{-2}	Log i_{corr}	Log (i_{corr}/T)	ΔG^*/ kJ.mol^{-1}	ΔH^*/ kJ.mol^{-1}	ΔS^*/J.K^{-1}.mol^{-1}	Ea/kJ.mol^{-1}	A Molecules. $cm^{-2}.S^{-1}$
Blank	298	0.0033	82.67	1.917	-0.557	62.104	15.318	-157.41	17.941	$6.4*10^{28}$
	308	0.0032	112.48	2.051	-0.437	63.674				
	318	0.0031	130.50	2.115	-0.387	65.244				
	328	0.0030	161.68	2.208	-0.307	66.814				
$2.7*10^{-6}$	298	0.0033	34.43	1.537	-0.937	64.328	35.422	-97.68	38.045	$8.4*10^{31}$
	308	0.0032	73.03	1.863	-0.625	65.298				
	318	0.0031	95.17	1.978	-0.524	66.268				
	328	0.0030	145.06	2.161	-0.354	67.238				
$1.3*10^{-5}$	298	0.0033	18.80	1.274	-1.200	65.908	46.240	-66.517	48.863	$3.5*10^{33}$
	308	0.0032	51.01	1.707	-0.781	66.568				
	318	0.0031	76.41	1.883	-0.619	67.228				
	328	0.0030	116.52	2.066	-0.449	67.888				
$2.7*10^{-5}$	298	0.0033	11.40	1.057	-1.417	67.262	53.554	-46.46	56.178	$3.9*10^{34}$
	308	0.0032	34.20	1.534	-0.954	67.722				
	318	0.0031	56.61	1.753	-0.749	68.182				
	328	0.0030	91.71	1.962	-0.553	68.642				
$4.1*10^{-5}$	298	0.0033	19.68	1.294	-1.180	65.828	37.816	-93.94	40.439	$1.3*10^{32}$
	308	0.0032	50.59	1.704	-0.784	66.768				
	318	0.0031	59.32	1.773	-0.729	67.708				
	328	0.0030	94.52	1.975	-0.540	68.648				

Table (4) shows, that the values of activation energy are highest in the presence of the inhibitor than for case in the absence of it, and the highest value obtained with the (N.C) concentration of ($2.7*10^{-5}$) M which equal to 56.178 kJ.mol^{-1}, in the other hand, the pre-exponential factor (A) was increase with adding (N.C).

Values of the enthalpy of activation for the corrosion process in the presence of (N.C) inhibitor are higher than for case in the absence of it, and the highest value obtained with $2.7*10^{-5}$ M (N.C) concentration which equal to 53.554 kJ. mol^{-1}.

Values of the entropy of activation ΔS^* for the corrosion of C.S process were slightly affected when (N.C) inhibitor was added.

The Gibbs free energy of activation values increase with temperature increase in the presence and absence of the inhibitor, and the highest values obtained with $2.9*10^{-6}$ M inhibitor concentration which increase from -67.262 kJ.mol^{-1} at 298 K to -68.642 kJ.mol^{-1} at 328 K.

3.3. Adsorption Isotherm

It is important to distinguish the best adsorption isotherm for the inhibitor adsorption process on metal surface because corrosion inhibition depend mostly on adsorption method of the inhibitor and conditions of the surface. The surface coverage (θ) calculation is done by (θ= IE/100), which the inhibition efficiency is directly proportion to the surface coverage , in the other hand, corrosion process is happened on the uncovered area only [15].

There are numerous isotherm of adsorption process (Temkin, Frumkin, Langmuir, Freundlich) were experienced, the best description was obtained with Langmuir adsorption isotherm, which assumed:

1. There are a constant number of adsorption sites on metal surface.
2. Every site catch only one adsorbate.
3. All sites have the same ΔG value and it do not depend on θ.
4. There are no reaction happened with one adsorbate to another, in other word, ΔG do not effected by adsorbate lateral interactions [16].

The following equation gives the Langmuir isotherm [17]:

$$C/\theta = 1/K_{ads} + C \qquad \ldots.(7)$$

Where C is the inhibitor concentration in mol.L^{-1}, K_{ads} is the equilibrium constant of the adsorption process and θ is the surface coverage.

Values of K_{ads} is obtained from the inverted value of the intersection point of the C/θ vs. C plot (figure 7) . If the correlation coefficient R^2, almost equal to 1, This mean that the inhibitor in this study obey the Langmuir isotherm.

The K_{ads} values may be taken as a measure of the strength of the adsorption forces between the inhibitor molecules and the metal surface [18].

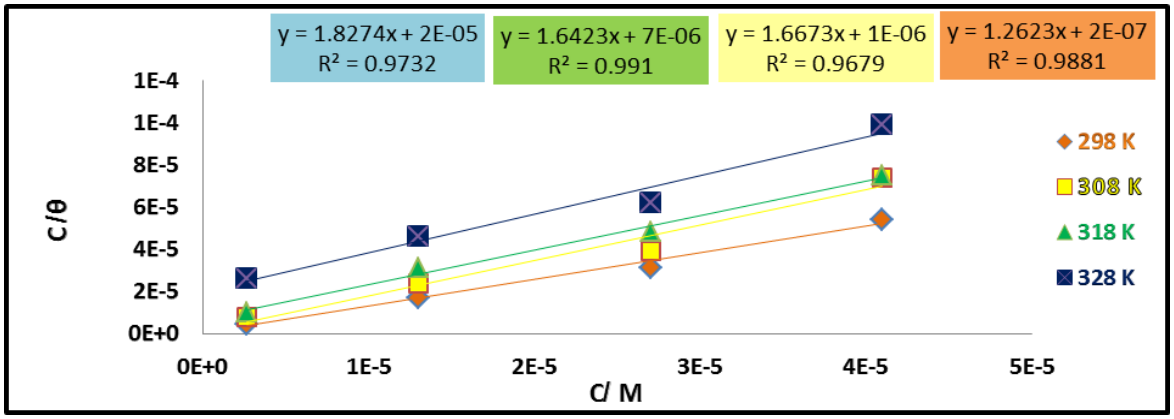

Figure 7. Langmuir isotherms plots for the adsorption of (N.C) on (C.S.) at different temperature.

Values of the enthalpy and the entropy of adsorption process had been determined from the following equation [19]:

$$\textbf{Log } K_{ads} = \frac{-\Delta H_{ads}}{2.303RT} + \frac{\Delta S_{ads}}{2.303R} + \textbf{Log } \frac{1}{55.55} \quad \textbf{.... (8)}$$

In the above equation, value of 55.55 is referred to the water concentration in unite of mol. L^{-1}.

Figure (8) shows the plot of log K_{ads} vs. 1/T, in which the value of ΔH_{ads} is obtained from the slope ($-\Delta H_{ads}/2.303R$) of the plot and value of ΔS_{ads} is obtained from the intercept of [(ΔS_{ads} /2.303R) +(log 1/55.55)] of the plot.

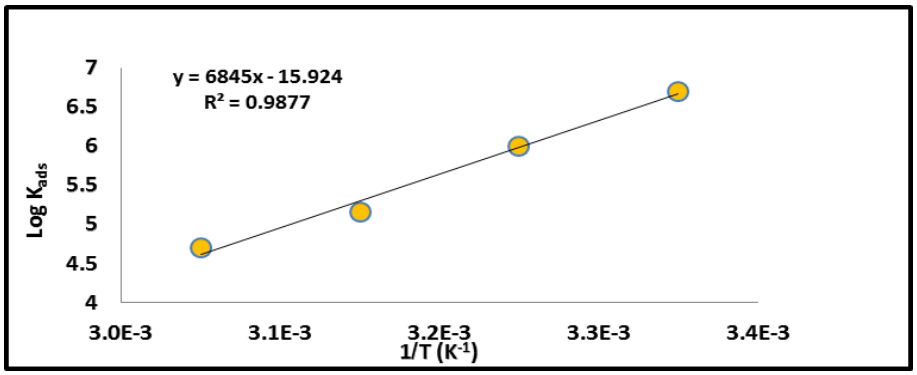

Figure 8. Plot of log K_{ads} versus 1/T.

Since ΔH_{ads} and ΔS_{ads} have been calculated, the values of free energy of adsorption can be easily calculated from equation (9).

$$\Delta G_{ads} = \Delta H_{ads} - T\,\Delta S_{ads} \text{ .... (9)}$$

The thermodynamic parameter from adsorption process was listed in table (5):

Table 5. Adsorption parameter for the (N.C) adsorption C.S surface.

T/K	K_{ads}/M^{-1}	$\Delta G/KJ.mol^{-1}$	$\Delta H/kJ.mol^{-1}$	$\Delta S/kJ.mol^{-1}.K^{-1}$	R^2
298	5,000,000	-50.302	-131.06	-271.51	0.9881
308	1,000,000	-47.592			0.9679
318	142,857.14	-44.882			0.9910
328	50,000	-42.172			0.9732

Table (5) shows, The highest value of K_{ads} obtained at 298 K which equal to 5 $*10^6$ M^{-1}, the negative value of the ΔH_{ads} indicated that the adsorption process of inhibitor is an exothermic process and it is equal to -131.06 $kJ.mol^{-1}$, since the negative value of ΔH_{ads} highest than -40 $kJ.mol^{-1}$ that's mean the adsorption of (N.C) inhibitor on C.S surface is an chemisorption process [20].

The negative value of the free energy of adsorption indicate a spontaneous adsorption of (N.C) inhibitor on C.S surface and decrease as the temperature increase.

3.4. FTIR Spectra

Figure (9A,B) shows the FTIR spectra for (N.C) powder and adsorbed inhibitor layer formed on C.S surface.

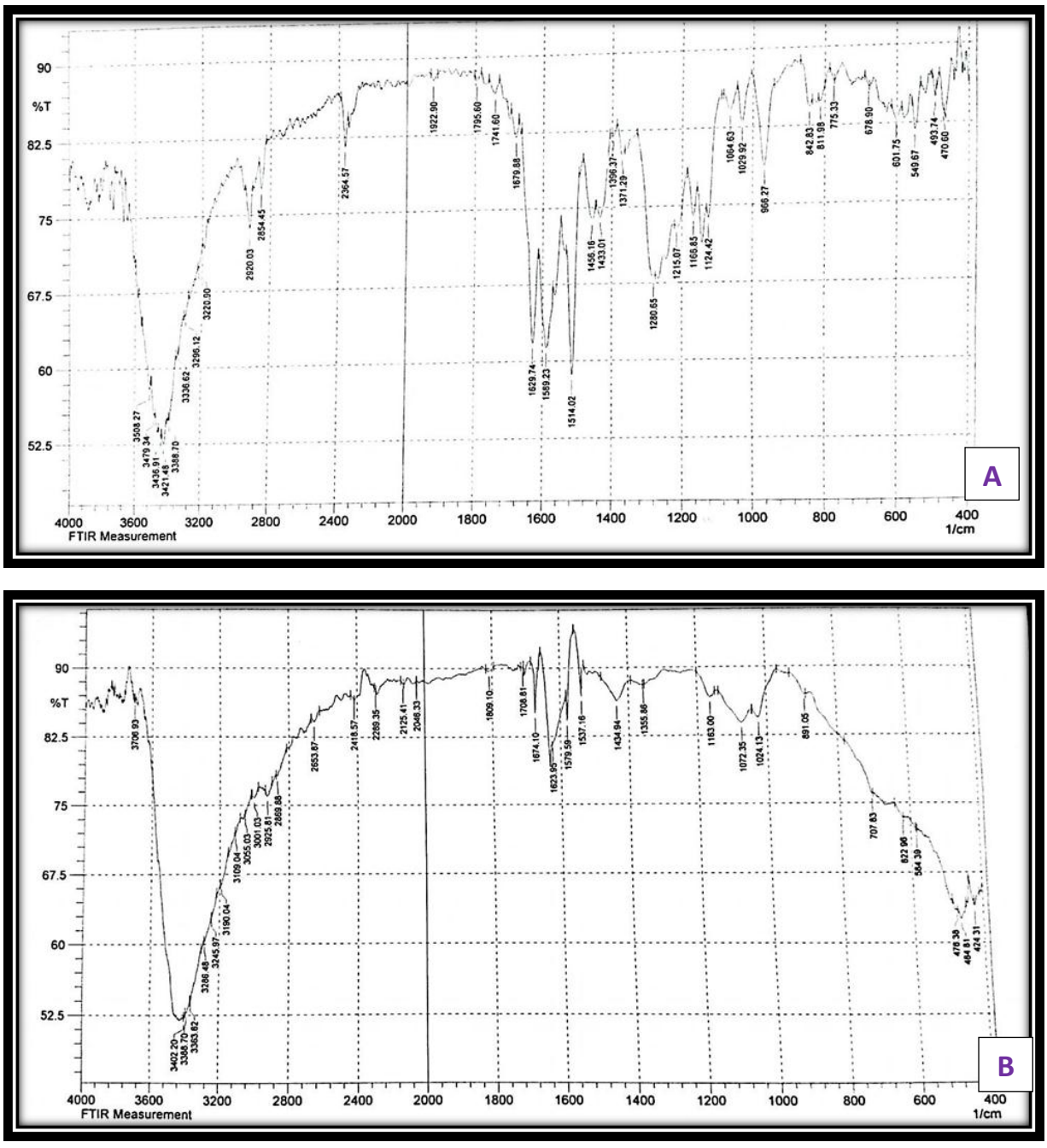

Figure 9. FTIR spectra of (N.C) inhibitor A) inhibitor powder, B) adsorbed inhibitor layer on C.S surface.

Table (6) shows the (N.C) functional groups and it's frequencies that have been appeared in figure (9A,B).

Table 6. FTIR functional group and frequencies for (N.C).

Functional groups	Frequencies of inhibitor powder (cm^{-1})	Frequencies of adsorbed inhibitor layer on C.S surface
OH (phenolic)	3421	3402 (shifting)
C-H (aliphatic)	2854,2920	2869,2925 (shifting)
C-H (aromatic)	3000	3001
C-H (alkenes)	3110	3109
C=C (aromatic)	1514,1589,1629	1537,1579,1623 (shifting)
C=C (aliphatic)	1679	1674

C=O (ketone)	1741	1708 (shifting)
C-O-C (asymmetric)	1280 [108]	disappear
C-O (alcoholic)	1166	1163
C-O-C (symmetric)	1140 [108]	1072 (shifting)

Table (6) shows the shifted and disappeared peaks when comparing between inhibitor powder and adsorbed inhibitor layer on C.S surface, which includes the slightly shifted peaks (phenolic O-H, aliphatic C-H and aromatic C=C) and strongly shifted ketonic C=C peak and symmetrical stretch C-O-C peak for ether, in the other hand, it's important to notice the disappearance of asymmetrical stretch (C-O-C) peak in the adsorbed inhibitor layer after it appearance in the (N.C) powder .

The above changes in the frequencies of the peaks are caused by the chemical reactions between the C.S surface and the inhibitor in the solution because of chemical adsorption nature of this inhibitor on C.S surface (depending on the clarification above in adsorption isotherm).

4.5. Surface Morphology AFM Studies

Surface morphology of (N.C) powder and the adsorbed inhibitor layer formed on carbon steel surface were studied through AFM technique.

Figure (10) and (11) shows the results of surface morphology analysis by AFM.

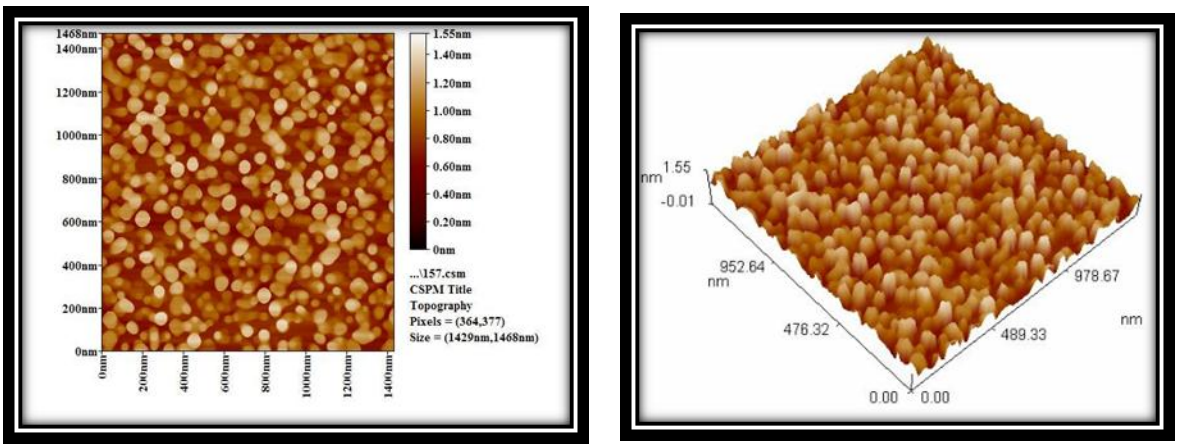

Figure 10. 2D and 3D views of AFM image of (N.C) powder.

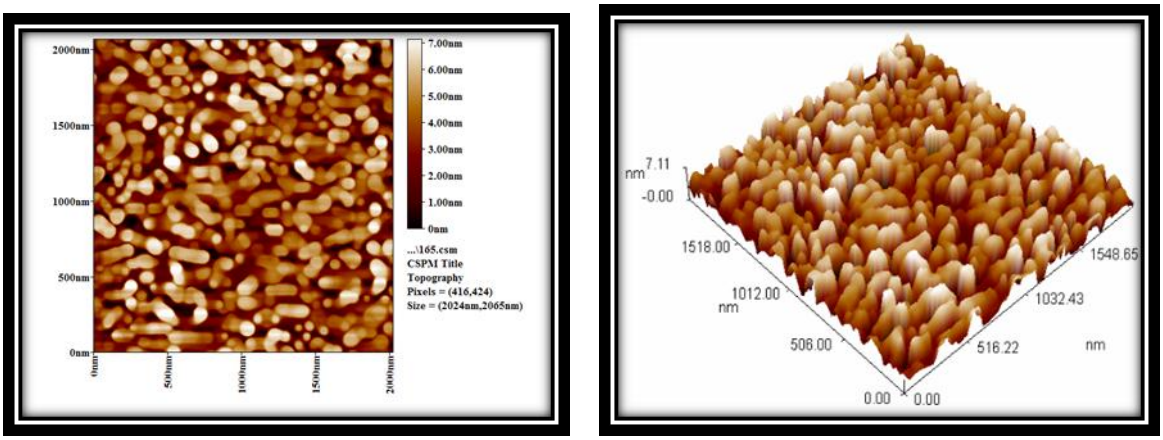

Figure 11. 2D and 3D views of AFM image of (N.C) adsorbed layer on C.S surface.

For (N.C) powder, the average roughness was calculated which equal to 40.55 nm, (figure 12), which was lower than the average roughness of adsorbed inhibitor layer formed on C.S surface that equal to 70.00 nm, (figure 13).

It mean's that the protected layer appear with particle size more than it before used (as powder).

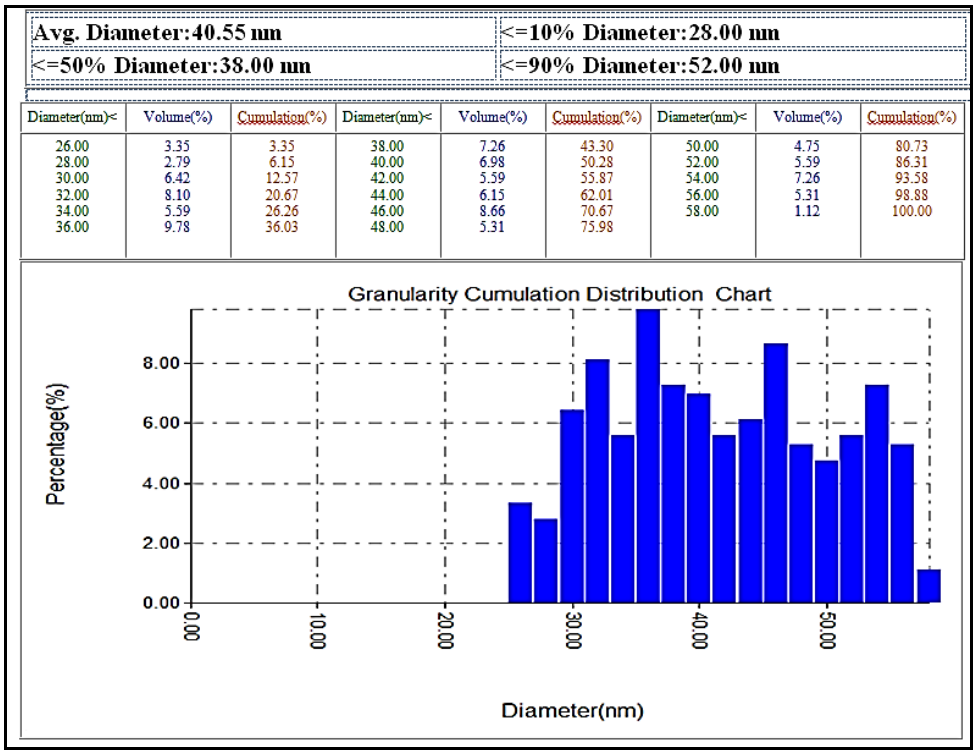

Diameter(nm)<	Volume(%)	Cumulation(%)	Diameter(nm)<	Volume(%)	Cumulation(%)	Diameter(nm)<	Volume(%)	Cumulation(%)
26.00	3.35	3.35	38.00	7.26	43.30	50.00	4.75	80.73
28.00	2.79	6.15	40.00	6.98	50.28	52.00	5.59	86.31
30.00	6.42	12.57	42.00	5.59	55.87	54.00	7.26	93.58
32.00	8.10	20.67	44.00	6.15	62.01	56.00	5.31	98.88
34.00	5.59	26.26	46.00	8.66	70.67	58.00	1.12	100.00
36.00	9.78	36.03	48.00	5.31	75.98			

Figure 12. Nano curcumin powder granularity cumulation distribution chart and average diameter.

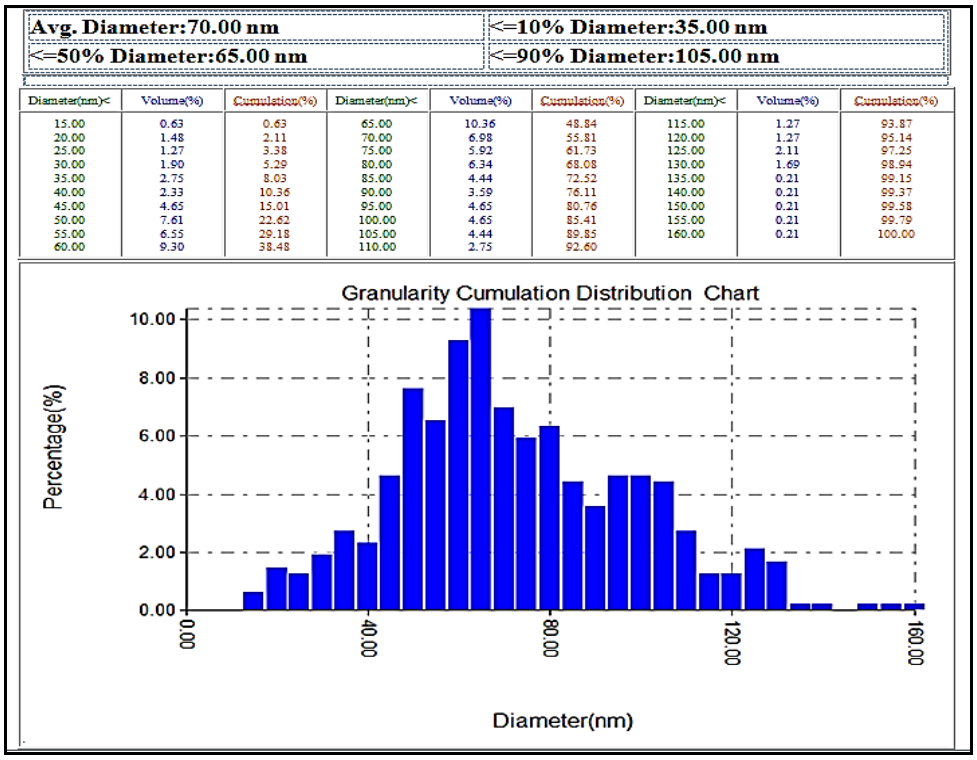

Diameter(nm)<	Volume(%)	Cumulation(%)	Diameter(nm)<	Volume(%)	Cumulation(%)	Diameter(nm)<	Volume(%)	Cumulation(%)
15.00	0.63	0.63	65.00	10.36	48.84	115.00	1.27	93.87
20.00	1.48	2.11	70.00	6.98	55.81	120.00	1.27	95.14
25.00	1.27	3.38	75.00	5.92	61.73	125.00	2.11	97.25
30.00	1.90	5.29	80.00	6.34	68.08	130.00	1.69	98.94
35.00	2.75	8.03	85.00	4.44	72.52	135.00	0.21	99.15
40.00	2.33	10.36	90.00	3.59	76.11	140.00	0.21	99.37
45.00	4.65	15.01	95.00	4.65	80.76	150.00	0.21	99.58
50.00	7.61	22.62	100.00	4.65	85.41	155.00	0.21	99.79
55.00	6.55	29.18	105.00	4.44	89.85	160.00	0.21	100.00
60.00	9.30	38.48	110.00	2.75	92.60			

Figure 13. Nano curcumin adsorbed layer on C.S surface granularity cumulation distribution chart and average diameter.

5. Conclusion

The inhibition efficiency decrease with temperature increase in the presence and absence of (N.C) inhibitor, and increase with inhibitor concentrations increase up to $2.7*10^{-5}$ M, then with increasing the inhibitor concentration more than $2.7*10^{-5}$ M, the inhibition efficiency will decrease and the highest value obtained with $2.7*10^{-5}$ M (N.C) concentration at 298 K which equal to 86.21%.

The polarization resistances in the presence of inhibitor are higher than for case in the absence of it, and the highest value obtained with $4.1*10^{-5}$ M at 298 K which equal to 903.72 $\Omega.cm^2$.

The corrosion potential values indicates that (N.C) inhibitor is a mixed type inhibitor (both anodic and cathodic) with some tendencies to become cathodic inhibitor at 318 and 328 K.

The activation energy are highest in the presence of the inhibitor than for case in the absence of it, and the highest value obtained with the (N.C) concentration of ($2.7*10^{-5}$) M which equal to 56.178 $kJ.mol^{-1}$, The same is happened with the pre-exponential factor (A) values which is increase with adding (N.C).

Values of the enthalpy of activation for the corrosion process in the presence of (N.C) inhibitor are higher than for case in the absence of it, and the highest value obtained with $2.7*10^{-5}$ M (N.C) concentration which equal to 53.554 kJ. mol^{-1}.

The values of Gibbs free energy of activation for corrosion process is increase with temperature increase in the presence and absence of the inhibitor.

The negative value of ΔH_{ads} indicated that the adsorption process of inhibitor is an exothermic process.

The negative value of the free energy of adsorption indicate a spontaneous adsorption of (N.C) inhibitor on C.S surface and decrease as the temperature increase.

The adsorption type of (N.C) on C.S surface is achemisorption type.

The best description of the adsorption process of (N.C) inhibitor on C.S surface is the Langmuir adsorption isotherm.

References:

1 . Winston Revie R. and H. Uhlig Herbert, Corrosion and Corrosion Control: An Introduction to Corrosion Science and Engineering, 4th ed., John Wiley & Sons, Inc., 2008,1.
2 . Al-Otaibi M. S., Al-Mayouf A. M., Khan M., Mousa A. A., Al Mazroa S. A. and Alkhathlan H. Z., Corrosion inhibitory action of some plant extracts on the corrosion of mild steel in acidic media, Arabian Journal of Chemistry, 2014,7, 340–346.
3 . Obot I.B., Obi-Egbedi N.O. and Umoren S.A., Antifungal drugs as corrosion inhibitors for aluminium in 0.1 M HCl, Corrosion Science,2009, 51, 1868-1875.
4 . Yıldırım A. and Çetin M., Synthesis and evaluation of new long alkyl side chain acetamide, isoxazolidine and isoxazoline derivatives as corrosion inhibitors, Corrosion Science, 2008, 50, 155-165.
5 . Javaherdashti Reza,Nwaoha Chikezie and Tan Henry, Corrosion and Materials in the Oil and Gas Industries, CRC Press, Taylor & Francis Group, LLC,2016**,**415.
6 . Basnet Purusotam and Skalko-Basnet Natasa, Review :Curcumin: An Anti-Inflammatory Molecule from a Curry Spice on the Path to Cancer Treatment, Molecules, 2011, 16, 4567-4598.
7 . Indira Priyadarsini Kavirayani, Review: The Chemistry of Curcumin: From Extraction to Therapeutic Agent, Molecules, 2014,19, 20091-20112.
8 . Ravichandran R., Pharmacokinetic Study of Nanoparticulate Curcumin: Oral Formulation for Enhanced Bioavailability, Journal of Biomaterials and Nanobiotechnology, 2013, 4, 291-299.
9 . Bisht Savita, Feldmann Georg, Soni Sheetal, Ravi Rajani, Karikar Collins, Maitra Amarnath and Anirban Maitra, Polymeric nanoparticle-encapsulated curcumin ("nanocurcumin"): a novel strategy for human cancer therapy, Journal of Nanobiotechnology, 2007, 5.

10 . Steffi P. F. and Srinivasan M., Preparation, Characterization and Stabilization of Curcumin Nanosuspension",International Journal of PharmTech Research, 2014, 6, 842-849.
11 . Srimathi M., Rajalakshmi R. and Subhashini S., Polyvinyl alcohol–sulphanilic acid water soluble composite as corrosion inhibitor formild steel in hydrochloric acid medium, Arabian Journal of Chemistry, 2010, 7, 647–656.
12 . McCafferty E., Introduction to Corrosion Science, Springer, New York, 2010.
13 . Ferreira E.S., Giacomelli C., Giacomelli F.C. and Spinelli A.,Evaluation of the inhibitor effect of l-ascorbic acid on the corrosion of mild steel,Materials Chemistry and Physics, 2004, 83,129–134,.
14 . Bilgic S. and Caliskan N., The effect of N-(1-toluidine) salicylaldimine on the corrosion of austenitic chromium–nickel steel, Appl. Surf. Sci., 1999, 152, 107-114.
15 . Umoren S. A., Li Y. and Wang F.H., Electrochemical Study of Corrosion Inhibition and Adsorption Behaviour for Pure Iron by Polyacrylamide in H_2SO_4: Synergistic Effect of Iodide Ions, Corros. Sci., 2010, 52, 1777–1786.
16 . Fouda A.S. and Elattar K.M., Curcumin Derivatives as Green Corrosion Inhibitors for α-Brass in Nitric Acid solution, JMEPEG, 2012, 21, 2354-2362.
17 . Hui C., Zhenghao F., Jinling S., Wenyan S. and Qi-X., Corrosion inhibitor of mild steel by aloes extract in HCl solution, International Journal of Electrochemical Science, 2013, 8, 720-734.
18 . DaBrowski A., Adsorption from Theory to Practice, Advance Colloid and Interface, 2001, 93, 135-224,.
19 . Salah S.A., Seta A. and Taobi H.A.A., Thermodynamic Properties of Amino Melamine Formaldehyde as Corrosion Inhibitor for Steel in Sulfuric Acid Solution, Mater. Environ. Sci., 2011, 2, 148–155.
20 . د. رحمة الله حسديه باقر هندسة, الـمعادن سطوح حمايـة و الـ تاكل, الـجامعة الـتكنولوجـية, الـمطابع الـ يمالـ, الـموصل في الـعالي, 1990, 83.

*****